Chapter 5

Propagation of shock wave in 2-D planar and axisymmetric non-ideal radiating gas flow under the influence of magnetic field *

"Great innovation only happens when
people aren't afraid to do things differently."

–Georg Cantor

* "The contents of this chapter is ***Communicated.***"

5.1 Introduction

In this chapter, we analyzed the influence of the magnetic field on the propagation of shock waves in radiation gasdynamics by using method of wavefront analysis. We examined the behavior of the waves propagated into the two-dimensional (2-D) steady supersonic magnetogasdynamic flow of non-ideal gas with radiation. The study of nonlinear phenomena is a prominent topic from mathematical as well as physical point of view because of its massive contribution in aerodynamics, space science, cosmology, rocket science, theory of relativity, interplanetary motion, and many more ([143, 144, 145]). In present scenario, many researchers and scientists are studying the theory of nonlinear waves with the help of partial differential equations describing the existence of these waves in certain mediums. The conservation laws of gas dynamics, electrodynamics, hydrodynamics, and other branches of mechanics are typically characterized by hyperbolic partial differential equations or system of such equations. Hyperbolic systems, in particular, represent the proper mathematical model for a variety of wave propagation phenomena [1].

Finding an analytical solution of system of the non-linear PDEs is a major challenge for researchers and scientists. While finding the solution of the system, the major problem is how to deal with non-linearity of the system and their physical interpretation. Therefore, for the analytical part of the solution, we must rely on some approximate analytical or numerical techniques to provide the necessary data for understanding the entire physical phenomenon. The main feature of the solutions to the nonlinear hyperbolic system resulting from conservation laws is wave breaking, which causes the development of the jump discontinuity propagated in the form of a shock wave [1]. The solution of these differential equations gives idea about the behavior of the waves propagating into the considered medium. Due to nonlinearity of PDEs, it is very difficult to obtain the solution of the problem. Many researchers

have studied the nonlinear waves in one dimensional system. When we look at two-dimensional problem, it becomes more complicated. In two-dimensional form it is very difficult to find the solution and the analysis of the study. For many years, shock wave theory has been used to explain the phenomena ranging from atomic explosions in the earth's atmosphere to supernova explosions and active galactic nuclei [97, 146]. Some authors have explored the analysis of shock wave propagation in the various gas regime and discussed the different physical features of these propagating waves [101, 147, 148]. Jagadeesh [96] has studied the various features of the shock wave theory, described the innovative shock wave applications in industries and science, and shown that the shock waves can enhance the temperature, pressure, and other flow variables experience rapid changes. Menon and Sharma [149] examined the flattening and steepening of characteristic wavefronts in planar and non-planar plasma motion in perfect gas and the magnetic field effect on wave propagation and have illustrated that the disturbance propagated into the medium obeys the Bernoulli-type differential equation. Whitham [150] have proposed a method to study the propagation and decay of weak shock wave produced by explosions and by the bodies in supersonic flight. The shock phenomena is most common in the interstellar medium. In stellar environments, shock waves often form due to collisions of photons with the electrons of the matter [151, 152]. The relativistic shock is an example of the astrophysical shock [153].

When the intensity of the electric field is much weaker than that of the magnetic field, then each of the electromagnetic quantities can be expressible in terms of the magnetic field and consider only the interaction between gas-dynamic field and magnetic field, the study of such phenomenon is known as magnetogasdynamics. The problem of a shock wave in a real gas with presence of magnetic field has been studied by many researchers in the past. In recent decades, many studies are available in

the literature on the propagation of magnetic shock waves and their applications in many industrial and scientific researches and developments. The propagation of waves and its behavior always depends on the flow variables and the medium chosen for the flow unless the motion of the wave need a medium for the flow. The strength of the wave depends on the Mach number, which is the ratio of the flow speed to the sound speed. Here, we consider the steady flow, therefore we do not consider the time dependence of the flow variables. In this chapter, we consider the transverse magnetic field; one may use an oblique shock wave to generalize this problem to get different results [154]. Pandey [155] has investigated the evolutionary process of the weak discontinuities and discussed the effect of magnetic field strength, and van der Waals excluded volume on the nature of the solution obtained by using the Lie group transformation. The study of two dimensional non-ideal gas flow under magnetic field effect is rarely described by authors in literature. The unsteady flow is described by many authors but only few studies are available in the literature on the steady flow of gas under the effect of magnetic field. Sharma et al. [156] have investigated the steady supersonic flow over a concave corner in radiative magnetogasdynamics. Pai and Speth [157] have derived the Rankine-Hugoniot relations for the normal shock wave in radiative magnetogasdynamics. Sahu [158] studied the propagation of cylindrical and spherical shock wave in a non-ideal gas with conductive as well as radiative heat fluxes in magnetogasdynamics under the presence of magnetic field.

The issues of radiative energy transmission in fluids stand out enough to be noticed in recent decades as a result of the speeding up bodies through the atmosphere and the extremely high temperatures achieved by gases in motion. Significant efforts have been made to study the interaction problems between the gasdynamic field and the radiation field, and a new title, Radiation Gasdynamics, has been proposed

for this subject. The new advancements in space innovation have necessitated an in-depth investigation of the consequences of the effect of thermal radiation on the flow field of extremely high-temperature gas. In many technological developments, such as space vehicle reentry, the temperature of the gas is so high that thermal radiation becomes a critical factor in determining the flow field. The effect of thermal radiation in gas dynamics is an excellent example of an interdisciplinary research activity that necessitates the practical application of the following crucial physical science fields: quantum mechanics, fluid mechanics, and statistical mechanics (with stress on quantitative spectroscopic investigations)[159, 160, 161]. The shock wave phenomenon is widespread in radiation gas dynamics because radiation effects are crucial in extremely high-speed flow, where shock waves usually occur. The phenomenon of the propagation of small disturbances in a radiating gas has been previously examined by [162, 163, 156, 164, 165]. Vincenti and Baldwin [166] studied the propagation of acoustic waves in a semi-infinite expanse of radiating gas on one side of an infinite plane radiating wall and investigated the disturbances that are caused in the gas by small sinusoidal oscillations in both the position and temperature of the wall. In past two decades, many researcher have used the method of wavefront analysis to study the wave propagation phenomena in different gas regime ([87, 167]). Singh et al. [67] used the wavefront analysis method to analyze the phenomenon of shock wave formation in a 2-D steady supersonic flow of a radiating gas and described the behavior of propagating waves and their flow patterns. Singh et al. [83] further examined the evolutionary process of shock wave propagation in non-ideal radiating gas. The basic equations governing the 2-D steady supersonic flow under the effect of radiative heat transfer modeled by van der Waals gas in magnetogasdynamics may be written as ([156])

$$\begin{cases} u\partial_x\varrho + v\partial_y\varrho + \varrho\left(\partial_x u + \partial_y v + \frac{mv}{y}\right) = 0, \\ \varrho u\partial_x u + \varrho v\partial_y u + (\partial_x p + \partial_x h) = 0, \\ \varrho u\partial_x v + \varrho v\partial_y v + (\partial_y p + \partial_y h) = 0, \\ u\partial_x p + v\partial_y p - \frac{\gamma p}{\varrho(1-b\varrho)}\left(u\partial_x\varrho + v\partial_y\varrho\right) + (\gamma-1)q = 0, \\ u\partial_x h + v\partial_y h + \varrho e^2\left(\partial_x u + \partial_y v + \frac{mv}{y}\right) = 0, \end{cases} \tag{5.1}$$

where x, y are spatial coordinates, ϱ is the density of the gas and u and v are the velocities in x and y direction, respectively. p represents the pressure and h is the magnetic pressure which is defined as $h = \frac{\omega H^2}{2}$. Here ω and H denotes the magnetic permeability and transverse magnetic field, respectively. q represents the rate of energy loss by the gas per unit volume through radiation and it is defined as $q = 4k\sigma(T^4 - T_b^4)$, where k is the Planck mean absorption coefficient is a function of density ϱ and temperature T of the gas. σ denotes the Stefan-Boltzmann constant and T_b is the uniform temperature of the body along which the flow is investigated. γ is the specific heat ratio of the gas. The energy loss $q = 4k\sigma T^4$, caused by the radiating gas has been enhanced by $q = -4k\sigma T_b^4$, resulting in an infinite optically thin gas with no radiating boundary. The boundary wall having uniform temperature T_b has no energy loss or gain due to the radiating gas. $e = (\frac{2h}{\varrho})^{\frac{1}{2}}$, is Alfvén speed. m is a constant such that $m = 0$ for planar flow and $m = 1$ for cylindrically axisymmetric flow.

The purpose of the present study is to analyze the simultaneous effect of magnetic field, radiative heat transfer and the imperfectness (non-idealness) of the gas on the flow pattern of the discontinuities propagated under the presence of magnetic field. It seems worthwhile to give a broader discussion of these effects for wave propagation problems in general and to investigate all the various possibilities that may arise. In this chapter, we study the behavior of the flow in ideal and non-ideal case and

compare the difference between the flow patterns and the physical changes took place.

The complete structure of this chapter is organized into sections as follows: In section 5.2 , we transform the basic equation into matrix form to determine the characteristic curves that represent the propagation of the waves. In the third section of this chapter, we introduce new coordinates and derive the transport equations, which describe the evolutionary process of the propagating waves. In section 5.4, we analyzed the behavior of the waves for plane and axisymmetric cases and determined the condition for the shock formation. Section 5.5 refers to the consequences of various parameter effects on the shock formation process and its deformation. The last section is the conclusion of the entire work of this chapter.

5.2 Characteristic formulation

In matrix form, equation (5.1) can be written as

$$V_x + MV_y + N = 0. \tag{5.2}$$

Here the subscript x and y signify the partial derivatives in x and y direction. V, N are column vectors and M is a square matrix of order 5 given below

$$V = \begin{pmatrix} \varrho \\ u \\ v \\ p \\ h \end{pmatrix}, \; N = \frac{1}{(u^2 - c^2)} \begin{pmatrix} \frac{\varrho muv}{y} + \frac{(\gamma-1)q}{u} \\ \frac{-mv}{y}c^2 - \frac{(\gamma-1)q}{\varrho} \\ 0 \\ \frac{\varrho muv}{y}a^2 + \frac{(\gamma-1)q}{u}(u^2 - e^2) \\ \frac{\varrho muv}{y}e^2 + \frac{(\gamma-1)q}{u}e^2 \end{pmatrix} \tag{5.3}$$

and the non-zero entries of the matrix $M = (M^{ij})_{5\times5}$ are as follows

$$\begin{cases} M^{11} = \frac{v}{u}, \quad M^{12} = -\frac{\varrho v}{(u^2-c^2)}, \quad M^{13} = \frac{\varrho u}{(u^2-c^2)}, \\ M^{14} = M^{15} = \frac{v}{u(u^2-c^2)}, \quad M^{22} = \frac{uv}{(u^2-c^2)}, \\ M^{23} = -\frac{c^2}{(u^2-c^2)}, \quad M^{24} = M^{25} = -\frac{v}{\varrho(u^2-c^2)}, \\ M^{33} = \frac{v}{u}, \quad M^{34} = M^{35} = \frac{1}{\varrho u}, \quad M^{42} = -\frac{\varrho v a^2}{(u^2-c^2)}, \\ M^{43} = \frac{\varrho u a^2}{(u^2-c^2)}, \quad M^{44} = \frac{v(u^2-e^2)}{u(u^2-c^2)}, \quad M^{45} = \frac{v a^2}{u(u^2-c^2)}, \\ M^{52} = -\frac{\varrho v e^2}{(u^2-c^2)}, \quad M^{53} = \frac{\varrho u e^2}{(u^2-c^2)}, \\ M^{54} = \frac{v e^2}{u(u^2-c^2)}, \quad M^{55} = \frac{v(u^2-a^2)}{u(u^2-c^2)}, \end{cases} \tag{5.4}$$

where $a = \left(\frac{\gamma p}{\varrho(1-b\varrho)}\right)^{\frac{1}{2}}$ is speed of sound for a non-ideal gas and $c = (a^2+e^2)^{\frac{1}{2}}$ is the magnetosonic speed.

Let μ^i denotes the eigen value of the matrix M and l^i denotes the corresponding left eigen vector, where $1 \le i \le 5$. Eigen values of M are given as

$$\mu^{(1,2)} = \frac{uv \pm c^2\left(\frac{M^2(1-b\varrho)}{\varepsilon} - 1\right)^{\frac{1}{2}}}{(u^2-c^2)}, \quad \mu^{(3,4,5)} = \frac{v}{u}. \tag{5.5}$$

Here, $M = \frac{(u^2+v^2)^{\frac{1}{2}}}{d}$ represents the upstream flow Mach number, b is the parameter of non-idealness and $d = \left(\frac{\gamma p}{\varrho}\right)^{\frac{1}{2}}$ is the speed of sound for ideal gas. The Alfvén number ε is defined as $\varepsilon = 1 + \frac{e^2}{a^2}$, which is 1 for non-magnetic case and greater than 1 for magnetic case.

The left eigen vectors l^i of the corresponding eigen values μ^i are given as

$$\begin{cases} l^{(1)} = \left(0 \quad 1 \quad -\frac{u}{v} \quad -\frac{1}{\varrho v}\left(\frac{M^2(1-b\varrho)}{\varepsilon} - 1\right)^{\frac{1}{2}} \quad 0\right), \\ l^{(2)} = \left(0 \quad 1 \quad -\frac{u}{v} \quad \frac{1}{\varrho v}\left(\frac{M^2(1-b\varrho)}{\varepsilon} - 1\right)^{\frac{1}{2}} \quad 0\right), \\ l^{(3)} = \left(1 \quad 0 \quad 0 \quad -\frac{1}{a^2} \quad 0\right), \\ l^{(4)} = \left(0 \quad 1 \quad \frac{v}{u} \quad \frac{\varepsilon}{\varrho u} \quad 0\right), \\ l^{(5)} = \left(0 \quad 0 \quad 0 \quad (1-\varepsilon) \quad 1\right). \end{cases}$$

Equation (5.5) shows that all eigen values of the matrix M are real for supersonic flow (M>1), therefore system (5.2) is hyperbolic in nature. Also, from equation (5.5), it can be notice that system (5.2) have two families of characteristic curves along $\frac{dy}{dx} = \frac{uv \pm c^2\left(\frac{M^2(1-b\varrho)}{\varepsilon}-1\right)^{\frac{1}{2}}}{(u^2-c^2)}$, that represents the waves propagating in opposite directions with the characteristic speed $\mu^{(1,2)}$.

5.3 Transport equations for the discontinuities

In this section, we shall derive the transport equations for the evolution of weak discontinuities in V as they move along the initial wavefront, which will be used for further study of the growth and decay behavior of shock wave. We assume that the initial wave front $\psi(x, y) = 0$, is described by the characteristic curve $\mu^{(1)}$ such that it passes through the point (x_0, y_0). Further, we consider that the initial wavefront $\psi(x, y) = 0$, moving with uniform velocity u_0 in x-direction and $v_0 = 0$ in y-direction, density ϱ_0, pressure p_0 and temperature $T_0 = T_b$. Here, we have used the suffix '0' to signify the value of the variables in the region ahead of the wavefront $\psi(x, y) = 0$. Now, we transform the coordinates x and y into curvilinear coordinates ψ and $\bar{y}$ by

using the following transformation ([6]):

$$\begin{cases} \psi_x + \mu^{(1)}\psi_y = 0, \\ \psi(x, y_0) = x - x_0, \\ y = \bar{y}. \end{cases} \tag{5.6}$$

Then ψ has the property that it is positive(negative) behind(ahead) of the leading characteristic on which $\psi = 0$.

Using the coordinate transformation (5.6) and multiplying equation (5.2) by $l^{(i)}$ from left side, (5.2) reduces into the following form

$$l^{(i)}V_\psi + \frac{\mu^{(1)}\mu^{(i)}}{\mu^{(1)} - \mu^{(i)}} x_\psi l^{(i)} V_{\bar{y}} + \frac{\mu^{(1)}}{\mu^{(1)} - \mu^{(i)}} x_\psi l^{(i)} N = 0, \tag{5.7}$$

where i is unsummed and $x_\psi = \frac{1}{\psi_x}$ is the jacobian of the transformation.

V and $V_{\bar{y}}$ are continuous across the wavefront $\psi(x, y) = 0$ and we use the subscript '0' to denote the values of V and $V_{\bar{y}}$ at the wavefront. On the other hand, V_ψ and x_ψ are discontinuous across the $\psi(x, y) = 0$. Evaluating equation (5.7) by putting the values of i $(i = 2, 3, 4, 5)$ behind the wavefront, we obtain

$$\varrho_\psi = \frac{1}{a_0^2} p_\psi, \tag{5.8}$$

$$u_\psi = -\frac{\varepsilon_0}{\varrho_0 u_0} p_\psi, \tag{5.9}$$

$$v_\psi = \frac{1}{\varrho_0 u_0} \left(\frac{M_0^2(1 - b\varrho_0)}{\varepsilon_0} - 1 \right)^{\frac{1}{2}} p_\psi, \tag{5.10}$$

$$h_\psi = (\varepsilon_0 - 1) p_\psi. \tag{5.11}$$

Taking $i = 1$ in (5.7) and differentiating with respect to ψ, then evaluating it behind the wavefront $\psi(x, y) = 0$, we get

$$c_0 a_0 \varepsilon_0^{\frac{1}{2}} \left(\frac{M_0^2(1-b\varrho_0)}{\varepsilon_0} - 1\right)^{\frac{1}{2}} p_{\psi\bar{y}} + u_0 \varrho_0 c_0 a_0 \varepsilon_0^{\frac{1}{2}} v_{\psi\bar{y}} + \frac{m u_0 \varrho_0}{\bar{y}} a_0^2 v_\psi + \frac{(\gamma-1)}{u_0}(u_0^2 - e_0^2) q_\psi = 0. \quad (5.12)$$

Equation of state for non-ideal gas is

$$p(1 - b\varrho) = \varrho RT, \quad (5.13)$$

where R is the gas constant. In view of (5.13), differentiating $q = 4k\sigma(T^4 - T_b^4)$ with respect to ψ and evaluating it behind $\psi = 0$, we obtain

$$q_\psi = \frac{16(\gamma-1)k\sigma T_b^4}{\varrho_0 a_0^2(1 - b\varrho_0)}. \quad (5.14)$$

Inserting the value of v_ψ and q_ψ from equation (5.10) and (5.14) in (5.12), we have

$$p_{\psi\bar{y}} + \left(\frac{m}{2\bar{y}} + \Phi\Theta_0\right) \varepsilon_0^{-1} p_\psi = 0, \quad (5.15)$$

where $\Phi = \frac{8(\gamma-1)k}{\Omega}$ denotes the measure of thermal radiation, $\Omega = \frac{\varrho_0 a_0^3}{(\gamma-1)\sigma T_b^4}$ represents the rate of the convective energy flux and $\Theta_0 = \frac{\varepsilon_0\left(\frac{M_0^2(1-b\varrho_0)}{\varepsilon_0} - 1\right) + 1}{M_0(1-b\varrho_0)^{\frac{1}{2}}\left(\frac{M_0^2(1-b\varrho_0)}{\varepsilon_0} - 1\right)^{\frac{1}{2}}}$.
Further, along $\psi = constant$, we have

$$x_{\bar{y}} = \frac{(u^2 - a^2\varepsilon)}{uv + a^2\varepsilon\left(\frac{M^2(1-b\varrho)}{\varepsilon} - 1\right)^{\frac{1}{2}}}. \quad (5.16)$$

Integrating equation (5.15) with respect to $\bar{y}$, we get

$$p_\psi = p_{\psi_0}\left(\frac{y_0}{\bar{y}}\right)^{\frac{m\varepsilon_0^{-1}}{2}} e^{\Phi\xi_0(y_0 - \bar{y})}, \quad (5.17)$$

where $\xi_0 = \Theta_0 \varepsilon_0^{-1}$ and p_{ψ_0} denotes the limiting value of p_ψ along $\psi = 0$ as $\bar{y} \longrightarrow y_0$. Taking derivative of (5.16) with respect to ψ and evaluating it behind the wavefront $\psi = 0$ and using (5.17), we obtain

$$x_{\psi\bar{y}} = \frac{2\varepsilon_0(1-\varepsilon_0) - (\gamma + \varepsilon_0 + \bar{b}(1-\varepsilon_0))M_0^2}{2\varrho_0\varepsilon_0 c_0^2 \left(\frac{M_0^2(1-\bar{b})}{\varepsilon_0} - 1\right)^{\frac{1}{2}}} \left(\frac{y_0}{\bar{y}}\right)^{\frac{m\varepsilon_0^{-1}}{2}} e^{\Phi\xi_0(y_0-\bar{y})} p_{\psi_0}, \tag{5.18}$$

where, $\bar{b}$ is defined as $\bar{b} = b\varrho_0$. Equation (5.15) and (5.18) are the transport equations for the discontinuities p_ψ and x_ψ, will be used to analyze the flow pattern and the behavior of the waves propagating into the disturbed region.

5.4 Behavior of the propagating waves

Integrating equation (5.18) with respect to $\bar{y}$, we have

$$x_\psi = 1 + \frac{2\varepsilon_0(1-\varepsilon_0) - (\gamma+\varepsilon_0+\bar{b}(1-\varepsilon_0))M_0^2}{2\varrho_0\varepsilon_0 c_0^2\left(\frac{M_0^2(1-\bar{b})}{\varepsilon_0}-1\right)^{\frac{1}{2}}} (y_0)^{\frac{m\varepsilon_0^{-1}}{2}} e^{\Phi\xi_0 y_0} p_{\psi_0} \int_{y_0}^{y} (z)^{-\frac{m\varepsilon_0^{-1}}{2}} e^{-\Phi\xi_0 z} dz. \tag{5.19}$$

In the above equation (5.19), we have used the boundary condition $x_{\psi-0} = x_\psi|_{\psi=0^-} = x_\psi|_{\psi=0^+} = 1$.

We consider $y = \kappa(x)$ to be the body contour equation in which the tangent to it remains parallel to the velocity of the streamline at the leading edge of the body. Along the stream line, we have

$$\frac{dy}{dx} = \frac{v}{u}. \tag{5.20}$$

Taking derivative of (5.20) with respect to ψ and evaluating it behind $\psi = 0$, we obtain

$$v_{\psi_0} = u_0 \kappa_0'', \tag{5.21}$$

where $\kappa_0^{''}$ is the curvature of the top of the body.

In view of (5.10) and (5.21), (5.19) can be written into the following form:

$$x_\psi = 1 + \frac{2\varepsilon_0(1-\varepsilon_0)-(\gamma+\varepsilon_0+\bar{b}(1-\varepsilon_0))M_0^2}{2\varepsilon_0\left(M_0^2(1-\bar{b})-\varepsilon_0\right)}\,(y_0)^{\frac{m\varepsilon_0^{-1}}{2}}\,M_0^2(1-\bar{b})\kappa_0^{''}e^{\Phi\xi_0 y_0}\int_{y_0}^{y}(z)^{-\frac{m\varepsilon_0^{-1}}{2}}\,e^{-\Phi\xi_0 z}dz. \tag{5.22}$$

In equation (5.22), since x_ψ is the jacobian of the transformation just behind $\psi = 0$, so that if for some $y = y_z$, jacobian vanishes, then the neighboring characteristics of the family $\psi = constant$ will intersect on the wavefront $\psi = 0$ and this will cause to develop a discontinuity in the solution V of the system (5.2) in the form of a shock wave. In this case, if we consider V_ψ is finite at $y = y_z$ as $x_\psi = 0$, then just behind the wavefront $\psi = 0$, $V_x = \frac{V_\psi}{x_\psi}$ will be infinite, which describes the wave propagation phenomenon.

Now, we shall discuss the significance of equation (5.22) and describe the supersonic flow of discontinuities propagated into the medium and its behavior for different values of m i.e., $m = 0$ for plane beak case and $m = 1$ for sharp edged ring case. This phenomenon has been shown in Fig.5.1.

Case I. Planar flow (m=0):

For $m = 0$, equation (5.22) takes the form:

$$x_\psi = 1 - \frac{\kappa_b^{''}(0)}{\Lambda}\left[1 - e^{-\Phi\xi_0(y-y_0)}\right], \tag{5.23}$$

where

$$\Lambda = 2\Phi\xi_0\varepsilon_0\left[M_0^2(1-\bar{b})-\varepsilon_0\right]\left[(\gamma+\varepsilon_0+\bar{b}(1-\varepsilon_0))M_0^2 - 2\varepsilon_0(1-\varepsilon_0)M_0^2(1-\bar{b})\right]^{-1} > 0$$

and $\kappa_b^{''}(0)$ stands for the value of the radius of curvature at the tip of the body, where the contour of the body starts bending. As we earlier mention that the formation

of shock depends on the jacobian x_ψ, i.e., when x_ψ vanishes, shock will form. From equation (19), it is clearly observed that x_ψ will vanish on the leading wavefront for $y_0 < y$ is possible only when $\kappa_b^{''}(0) > 0$ with $\kappa_b^{''}(0) > \Lambda$. When $\kappa_b^{''}(0) \leq \Lambda$, this is the case where x_ψ remains positive for $y_0 < y$ and resulting from that, the shock formation is not possible on the leading wavefront. Thus, we see that Λ plays an important role in shock formation. It represents a critical level in such a manner that whenever the radius of curvature $\kappa_b^{''}(0)$ surpasses this level at the tip of the body, shock will form at a finite distance far from the body.

Now, at the wavefront $x_\psi = 0$, we have $v_x = \frac{v_\psi}{x_\psi}$. From equation (5.8), (5.14) and (5.23) for $m = 0$, we obtain

$$v_x = \frac{c_0 M_0 (1-\bar{b})^{\frac{1}{2}} \kappa_b^{''}(0) e^{-\Phi\xi_0(y-y_0)}}{\varepsilon_0^{\frac{1}{2}} \left[1 - \frac{\kappa_b^{''}(0)}{\Lambda}(1 - e^{-\Phi\xi_0(y-y_0)})\right]}. \tag{5.24}$$

Equation (5.24) describes the evolutionary process of the propagating waves. Since, for $\kappa_b^{''}(0) > 0$ with the condition $\kappa_b^{''}(0) > \Lambda$, shock will form and the corresponding shock formation distance $y = y_z$ is given by

$$y_z = y_0 + \frac{1}{\Phi\xi_0} \log\left\{\frac{\kappa_b^{''}(0)}{\kappa_b^{''}(0) - \Lambda}\right\}. \tag{5.25}$$

In the above equation (5.24), the denominator becomes zero while the numerator remains finite, indicating that the velocity gradient at the wavefront $\psi = 0$ becomes unbounded at a distance $y = y_z$, resulting in that the wave terminates into a shock wave. Equation (5.25) shows that this behavior coincides with the vanishing of x_ψ. The wave remains compressive in case $\kappa_b^{''}(0) \leq \Lambda$, but the velocity gradient does not steepen. In contrast, v_x along the wavefront $\psi = 0$ diminishes or it becomes stationary according as $\kappa_b^{''}(0) < \Lambda$ or $\kappa_b^{''}(0) = \Lambda$, respectively and in this case shock will not form on the leading wavefront $\psi = 0$.

Case II. Axisymmetric flow (m=1):

In this case, we consider that $y = y_z(x)$ represents a ring-shaped body with a sharp-edged inlet, which initiates the initial perturbation running both inwards and outwards along the characteristic lines.

For $m = 1$, equation (5.22) can be rewritten as

$$x_\psi = 1 - \frac{\left[-2\varepsilon_0(1-\varepsilon_0)+(\gamma+\varepsilon_0+\bar{b}(1-\varepsilon_0))M_0^2\right]}{2\varepsilon_0\left(M_0^2(1-\bar{b})-\varepsilon_0\right)}(y_0)^{\frac{\varepsilon_0^{-1}}{2}} M_0^2(1-\bar{b})\kappa_z''(0)e^{\Phi\xi_0 y_0}\pi, \tag{5.26}$$

where $\pi = \int_{y_0}^{y}(z)^{-\frac{\varepsilon_0^{-1}}{2}} e^{-\Phi\xi_0 z}dz$. It is clear from equation (5.26) that for $y > y_0$, the quantity within the square bracket is always positive and less than one. As a result, if $\kappa_z''(0)$ is positive and exceeds the critical value π^{-1}, the jacobian x_ψ will vanish, resulting in the formation of shock. On the other hand, if $\kappa_z''(0) \leq \pi^{-1}$, the value of x_ψ will always be greater than one, indicating that no shock will ever form on the leading wavefront. Table 5.1 and 5.2 shows the value of π for magnetic and non-magnetic case for different values of Φ respectively.

γ	ε_0	$\bar{b}$	M_0^2	Φ	π
1.4	1.6	0.0	2.5	0.8	0.173668
				1.0	0.135855
				1.2	0.106363
			3.5	0.8	0.193949
				1.0	0.125398
				1.2	0.155901
1.4	1.6	0.1	2.5	0.8	0.160981
				1.0	0.123606
				1.2	0.949981
			3.5	0.8	0.189555
				1.0	0.151512
				1.2	0.121186

TABLE 5.1: Variation in the value of π for magnetic ideal and non-ideal case.

γ	ε_0	$\bar{b}$	M_0^2	Φ	π
1.4	1.0	0.0	2.5	0.8	0.126074
				1.0	0.920633
				1.2	0.067318
			3.5	0.8	0.140072
				1.0	0.104957
				1.2	0.0787336
1.4	1.0	0.1	2.5	0.8	0.119994
				1.0	0.0865711
				1.2	0.0625481
			3.5	0.8	0.136397
				1.0	0.101539
				1.2	0.075679

TABLE 5.2: Variation in the value of π for non-magnetic ideal and non-ideal case.

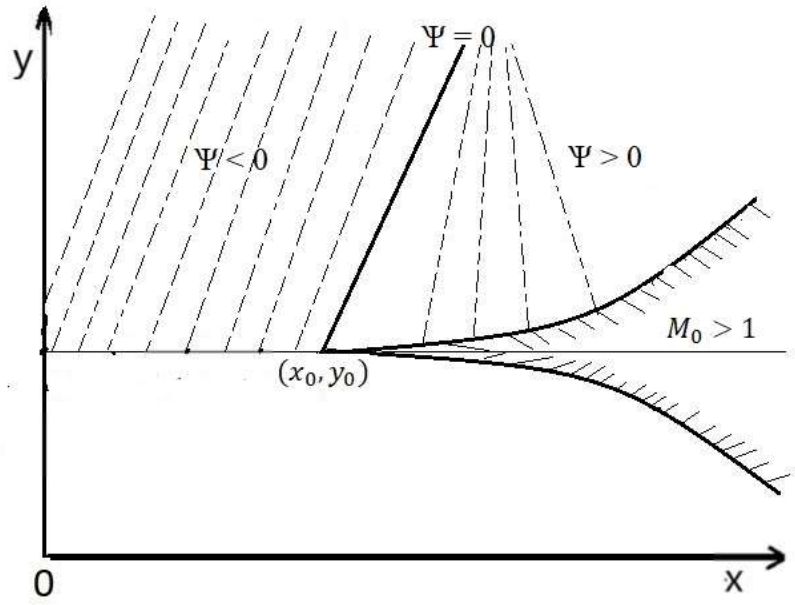

FIGURE 5.1: Convergence of the characteristics for supersonic planar and axisymmetric flow.

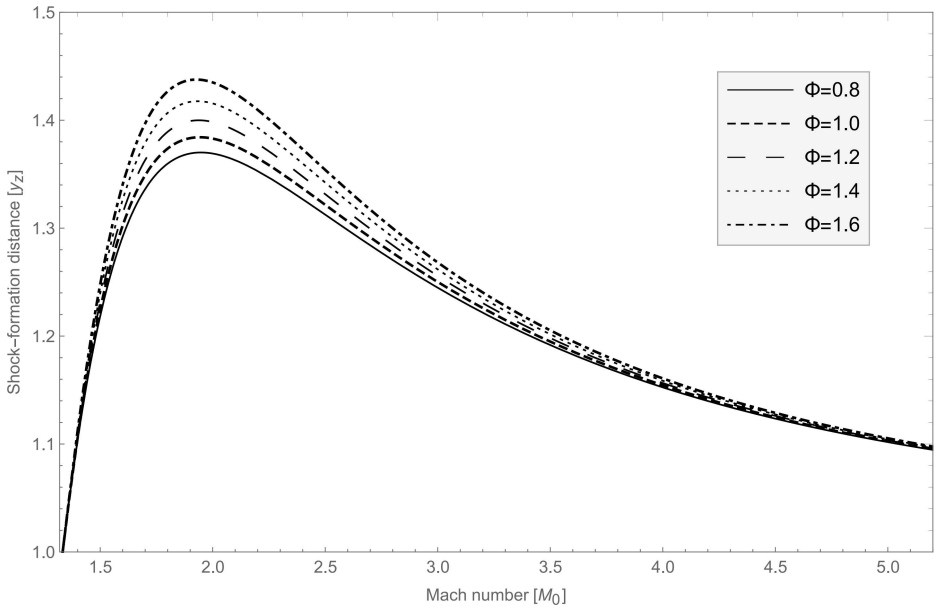

(a) Effect of thermal radiation on the shock formation distance for $\gamma = 1.4$.

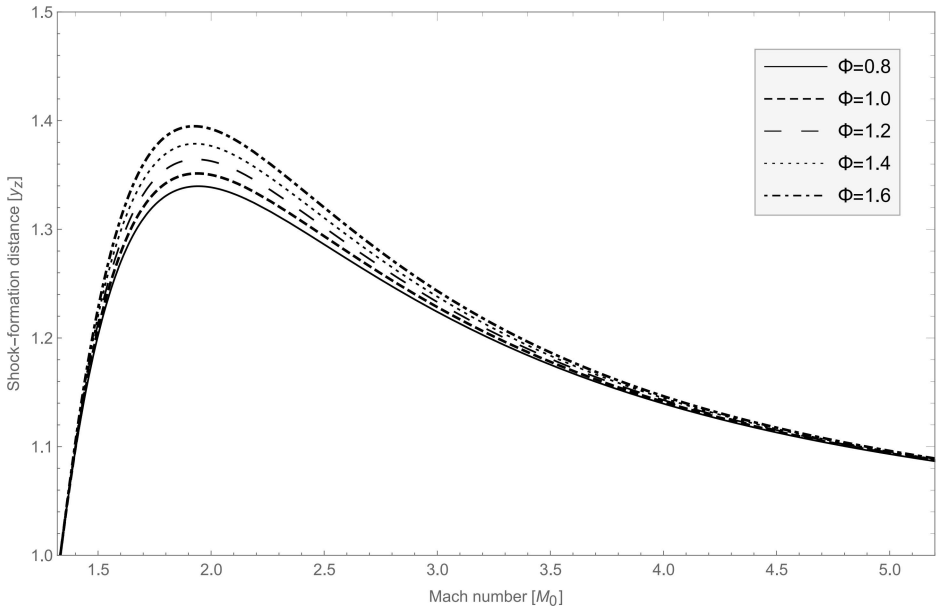

(b) Effect of thermal radiation on the shock formation distance for $\gamma = 1.67$.

FIGURE 5.2: Effect of thermal radiation on the shock formation distance with $\varepsilon_0 = 1.6$, $b = 0.1$.

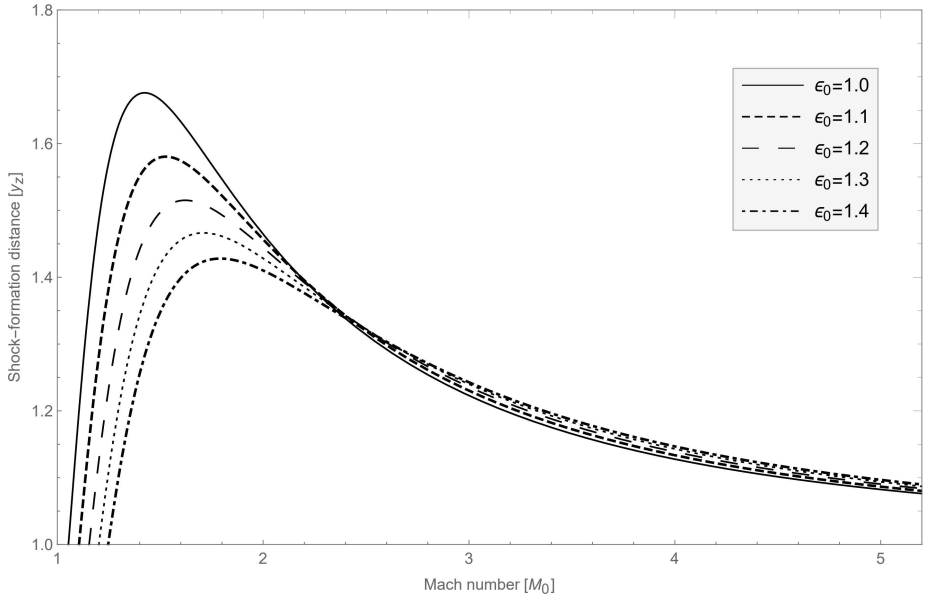

(a) Effect of magnetic field on the shock formation distance for $\gamma = 1.4$.

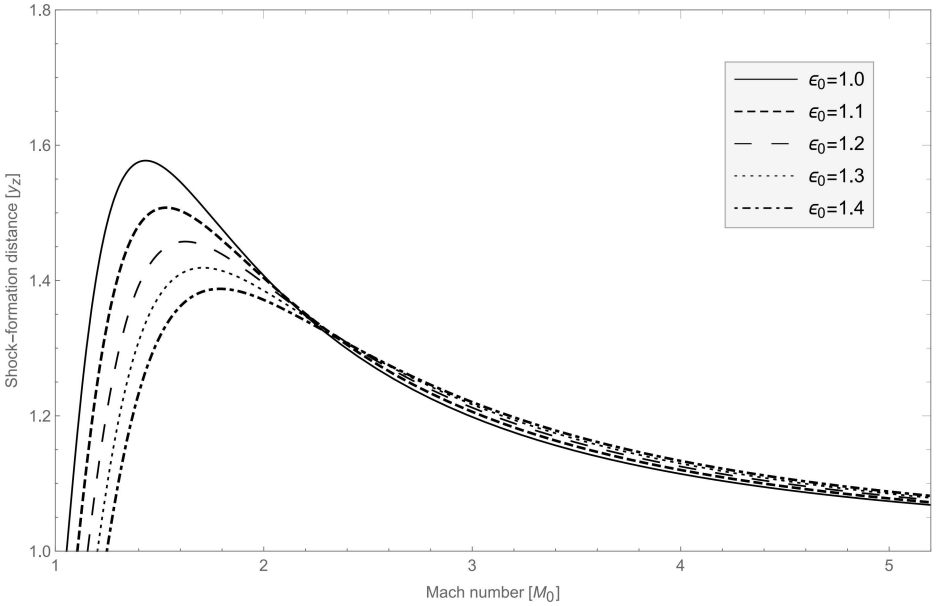

(b) Effect of magnetic field on the shock formation distance for $\gamma = 1.67$.

FIGURE 5.3: Effect of magnetic field on the shock formation distance with $\Phi = 0.8$, $b = 0.1$.

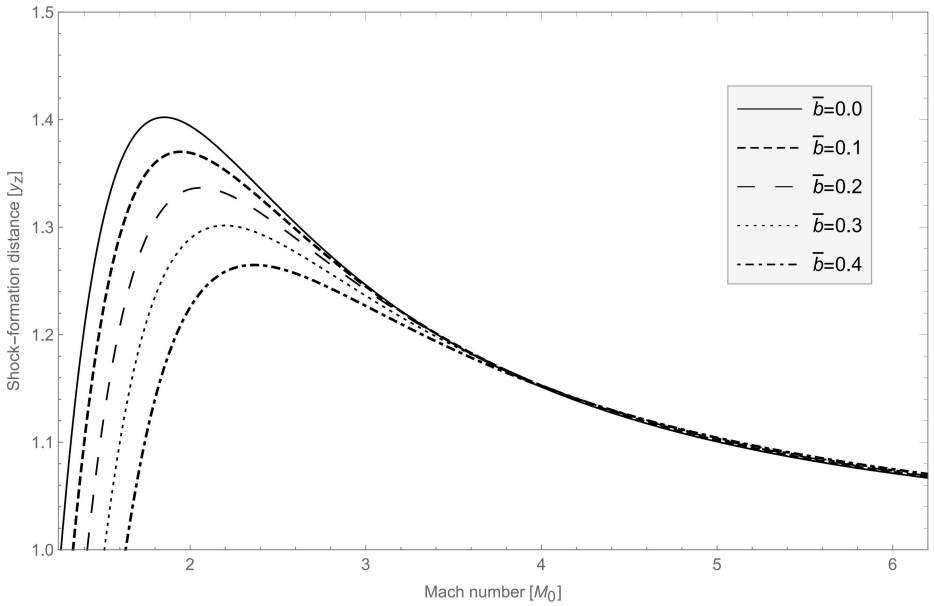

(a) Effect of non-ideal parameter b on the shock formation distance for $\gamma = 1.4$.

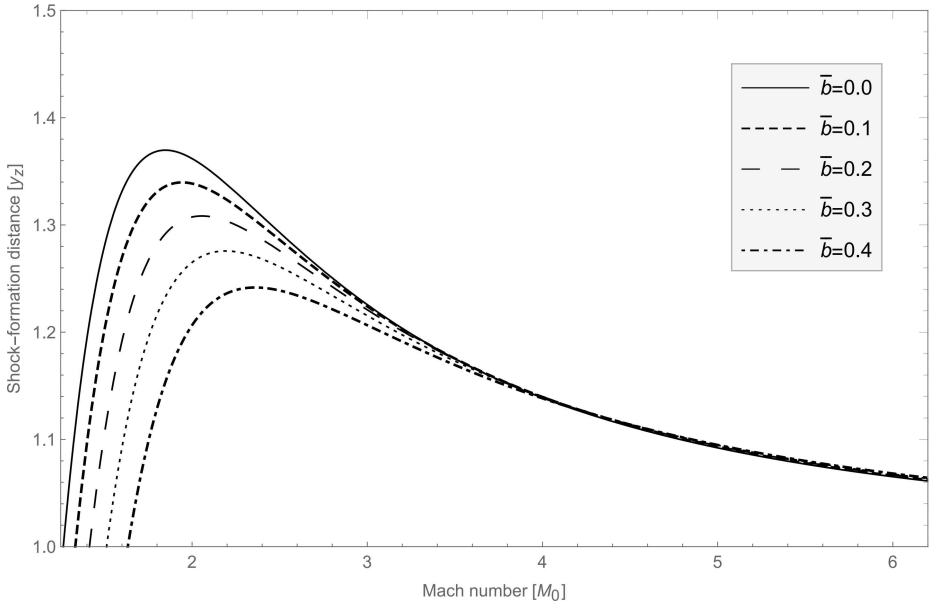

(b) Effect of non-ideal parameter b on the shock formation distance for $\gamma = 1.67$.

FIGURE 5.4: Effect of non-idealness on the shock formation distance with $\Phi = 0.8$, $\varepsilon_0 = 1.6$.

5.5 Results and discussion

In this section, we shall discuss the various parameter effects on the propagating waves and discuss the possibilities of shock formation for both the cases (plane beak case and sharp edged ring case). From (5.24), we see that for $M_0 \sim \varepsilon_0$, shock formation distance is given by

$$y_z \sim y_0 - \frac{2\left[\frac{M_0^2(1-\bar{b})}{\varepsilon_0} - 1\right]}{\left[(\gamma+\varepsilon_0+\bar{b}(1-\varepsilon_0))\varepsilon_0^2 - 2\varepsilon_0(1-\varepsilon_0)\right](1-\bar{b})},$$

whereas for $M_0 >> \varepsilon_0$,

$$y_z \sim y_0 - \frac{2\varepsilon_0}{\left[(\gamma+\varepsilon_0+\bar{b}(1-\varepsilon_0))M_0^2 - 2\varepsilon_0(1-\varepsilon_0)\right]}.$$

It can be observed from the above expression that the shock formation distance is a decreasing function of the Mach number M_0, i.e., if we increase the value of the Mach number, corresponding to this increment, shock formation distance decreases. Hence for increasing the value of the Mach number, the time for the shock formation will reduce.

Since $\kappa_b^{''}(0) < 0$ corresponds to the situation when the shape of the body has expansive corner at $x = 0$. Therefore for $|\kappa_b^{''}(0)| \geq \Lambda$, (5.24) yields

$$v_x = \frac{-2\Phi\xi_0\varepsilon_0^2 c_0\left[\frac{M_0^2(1-\bar{b})}{\varepsilon_0} - 1\right]}{\left[(\gamma+\varepsilon_0+\bar{b}(1-\varepsilon_0))M_0^2 - 2\varepsilon_0(1-\varepsilon_0)\right]M_0} \times \frac{e^{-\Phi\xi_0(y-y_0)}}{1-e^{-\Phi\xi_0(y-y_0)}}. \tag{5.27}$$

From equation (5.27), we can determine the velocity gradient at the head of a Prandtl-Meyer expansion flow.

5.5.1 Analysis of the effects of thermal radiation on the shock formation process.

In this section, we shall discuss the consequences of the effect of thermal radiation on the shock formation distance and investigate the evolutionary process of the propagating waves. Fig.5.2 depicts the effect of thermal radiation on the shock formation distance for (a) $\gamma = 1.4$ and (b) $\gamma = 1.67$. From Fig.5.2(a), we observe that as we increase the value of the parameter Φ, shock formation distance will increase and causes to increase in the time for the formation of the shock. Also, we notice that as the Mach number increases, the shock formation distance decreases, resulting in an early shock formation. Thus, the behavior of the propagation process under the thermal radiation effect and Mach number effect is opposite. A similar result can be seen from Fig.5.2(b), which shows the thermal radiation effect for $\gamma = 1.67$. If we compare the results shown in Fig.5.2(a) and 5.2(b), we observe that as we increase the value of γ, shock formation distance decreases, resulting in an early shock formation, i.e., y_z is a decreasing function of γ.

5.5.2 Analysis of an increase in the value of magnetic parameter ε_0.

Fig. 5.3(a) and Fig.5.3(b) shows the magnetic field effect on the shock formation distance for $\gamma = 1.4$ and $\gamma = 1.67$ respectively. Fig.5.3(a) reveals that an increase in the value of ε_0 enhances the shock formation distance. For non-magnetic case ($\varepsilon_0 = 1.0$), shock forms later as compared to magnetic case. Similarly, in Fig.5.3(b), we see that as we increase in the value of ε_0, shock forms earlier. Also, if we increase the value of γ, shock formation distance decreases,i.e., an increase in the value of the parameter γ causes to decrease in the time for shock formation. In Fig.5.3(a)

and 5.3(b), we found that the flatness of the curve increases with an increase in the Mach number. Thus, the behavior of the propagating waves under the effect of magnetic field and Mach number are the same, i.e., for increasing value of Mach number or magnetic field parameter ε_0, shock formation distance y_z decreases. In the non-magnetic case, shock formation distance y_z decreases rapidly as compared to the magnetic case.

5.5.3 Analysis of an increase in the value of non-ideal parameter $\bar{b}$.

Fig.5.4(a) and Fig.5.4(b) shows the effect of non-idealness on the shock formation distance for $\gamma = 1.4$ and $\gamma = 1.67$ respectively. In Fig.5.4(a), it can be noticed that an increase in the value of non-ideal parameter $\bar{b}$ causes to decrease the shock formation distance y_z,i.e., increase in the value of $\bar{b}$ reduces the time for shock formation. Fig.5.4(b) shows the similar phenomenon as observed from Fig.5.4(a), which is for $\gamma = 1.4$. Further, for increasing value of γ, y_z decreases and an early shock will form. Thus, we see that effect of magnetic field strength and the parameter of non-idealness are similar whereas in case of thermal radiation we get opposite results. Hence, we found that the an increase in the value of the parameter ε_0 or $\bar{b}$ causes to increase the formation process of the shock and increase in the value of Φ or Mach number M_0 enhances the shock formation distance.

5.6 Conclusion

The present study deals with the combined effect of non-idealness and the radiative heat transfer effect under the influence of magnetic field on the propagation of

shock wave. The optically thin approximation is treated for the effect of thermal radiation. We have described what physical changes takes place when we change (increase or decrease) the values of the parameters required for the motion. The fundamental differential equation (transport equations) governing the growth and decay of disturbances propagated into the medium is obtained using the wavefront analysis method, which determines the distance at which the characteristic curves intersect, and the conditions that ensure no shock will ever form on the wavefront. It is found that the shock formation completely relies on the upstream flow Mach number M_0, the magnetic field parameter ε_0 and initial body curvature η which may be either $\kappa_b^{''}(0)^{-1}$ or $\kappa_z^{''}(0)^{-1}$, non-ideal parameter b and Φ, which represents the importance of thermal radiation. It is observed that the presence of a magnetic field and non-idealness reduces the time for shock formation, i.e., increasing the magnetic field strength and the value of the non-ideal parameter causes shock to form earlier, whereas increasing the value of the Boltzmann number delays the formation process of shock.

****